ADOLESCENT BINGE DRINKING LEADS TO LONG-LASTING CHANGES IN CORTICAL MICROCIRCUITS

Avery R Sicher[1,2], William D. Starnes[2], Keith R. Griffith[2], Nigel C. Dao[2], Grace Smith[2,3], Dakota F. Brockway[1,2], Nicole A. Crowley[1,2,3,4,5]

1 Neuroscience Graduate Program, The Huck Institutes of the Life Sciences, University Park PA 16802

2 Department of Biology, Penn State University, University Park PA 16802

3 Department of Biomedical Engineering, Penn State University, University Park PA 16802

4 The Huck Institutes of the Life Sciences, Penn State University, University Park PA 16802

5 Center for Neural Engineering, Penn State University, University Park PA 16801

Correspondence to:
Nicole A. Crowley, PhD
Assistant Professor
Departments of Biology and Biomedical Engineering
Penn State University
326 Mueller Lab
University Park PA 16802
Tel: (814) – 863-0278
Email: nzc27@psu.edu
Website: www.crowley-lab.org

ABSTRACT

Adolescent drug consumption has increased risks to the individual compared to consumption in adulthood, due to the likelihood of long-term and permanent behavioral and neurological adaptations. However, little is known about how adolescent alcohol consumption influences the maturation and trajectory of cortical circuit development. Here, we explore the consequences of adolescent binge drinking on somatostatin (SST) neuronal function in the prelimbic (PL) cortex. We find that adolescent drinking-in-the-dark (DID) produces sex-dependent increases in intrinsic excitability of SST neurons, persisting well into adulthood. We found a complementary reduction in pyramidal neuron excitability immediately after binge drinking; however, this hypoexcitability rebounded towards increased pyramidal neuron activity in adulthood in females, suggesting long-term homeostatic adaptations in this circuit. Together, this suggests that binge drinking during key developmental timepoints leads to permanent changes in PL microcircuitry function, which may have broad behavioral implications.

1. INTRODUCTION

1.1 Adolescence and alcohol misuse

Adolescence is broadly defined as the transitional period between childhood and adulthood, marked by a variety of maturational changes throughout the body (Spear 2000). In the brain, the prefrontal cortex (PFC) is one of the last regions to finalize development, with a variety of morphological, functional, and neuromodulatory changes occurring throughout this period (Sicher et al., 2022). This critical and time-locked development may make the PFC a particularly vulnerable brain region to insults including alcohol use, as any events which interfere with typical PFC development may produce permanent and lifelong consequences. Unfortunately coinciding with this developmental window, adolescents are at a high risk of initiating drug and alcohol use. Alcohol consumption in adolescents often occurs as an episode of binge drinking, defined by the National Institute on Alcohol Abuse and Alcoholism (NIAAA) as a pattern of drinking which raises the blood ethanol concentration (BEC) above 80 mg / dL (NIAAA, 2021). In adult women and men, this typically requires 4 or 5 alcoholic drinks respectively within a 2 hr period; however, adolescents may reach BECs exceeding 80 mg / dL after consuming as few as 3 drinks due to their smaller body size (Donovan, 2009). The NIAAA estimates that around 90% of alcohol consumed by people under the age of 21 is consumed in an episode of binge drinking (NIAAA, 2021)– setting the stage for long-term consequences driven by the adolescent onset of alcohol consumption.

The risks and consequences of adolescent binge drinking are both acute and long-term. While acute risks include car accidents or alcohol poisoning, long-term consequences can include impaired development of the PFC. Studies in both rodent models and human adolescents have shown that alcohol consumption interferes with typical maturation of the prelimbic (PL) region of the PFC, potentially inducing permanent changes in PFC structure and corresponding behavioral aberrations (for review see Sicher et al., 2022). The effects of alcohol on the PL cortex seem to be age dependent, as alcohol consumption during early adolescence, but not early adulthood, increased the excitability of deep-layer cortical pyramidal neurons (Galaj et al., 2020). Similarly, alcohol consumption in adolescence altered medial PFC plasticity, causing persistent changes in fear extinction, whereas adult mice which consumed alcohol showed no behavioral changes (Lawson et al., 2022). This suggests critical windows for the interaction between development, drug exposure, and PFC circuits.

The risks and consequences of adolescent binge drinking are both acute and long-term. While acute risks include car accidents or alcohol poisoning, long-term consequences can include impaired development of the PFC. Studies in both rodent models and human adolescents have shown that alcohol consumption interferes with typical maturation of the prelimbic (PL) region of the PFC, potentially inducing permanent changes in PFC structure and corresponding behavioral aberrations (for review see Sicher et al., 2022). The effects of alcohol on the PL cortex seem to be age dependent, as alcohol consumption during early adolescence, but not early adulthood, increased the excitability of deep-layer cortical pyramidal neurons (Galaj et al., 2020). Similarly, alcohol consumption in adolescence altered medial PFC plasticity, causing persistent changes in fear extinction, whereas adult mice which consumed alcohol showed no behavioral changes (Lawson et al., 2022). This suggests critical windows for the interaction between development, drug exposure, and PFC circuits.

1.2 Prelimbic somatostatin neurons and drug use

Somatostatin (SST) is a neuropeptide which represents a promising target for substance use disorders and other neuropsychiatric conditions (Brockway and Crowley, 2020). SST is co-expressed in a major population of GABAergic neurons, with SST neurons representing about 20% of GABAergic neurons in the mouse frontal cortex (Xu et al., 2010). Little work thus far has characterized changes in SST neurons throughout development. SST neurons in the PL region of the PFC show an increase, followed by pruning during the early-to-mid stages of adolescence in female rodents (Du et al., 2018). Membrane properties of medial PFC (infralimbic and anterior cingulate cortex) SST neurons stabilize early in life, around the third postnatal week (Koppensteiner et al., 2019; Pan et al., 2016), though typical changes in the electrophysiological properties of prelimbic SST neurons during adolescence have not been studied.

Recent work has sought to understand the effects of alcohol on SST neurons. Our lab and others have demonstrated that SST neurons in the PL cortex are vulnerable to several paradigms of alcohol exposure in adult mice (Dao et al., 2021; Joffe et al., 2020). SST has also been identified as an important target of adult alcohol consumption, with SST gene expression underlying alcohol-induced changes in local circuitry and functional connectivity in humans (Ochi et al., 2022). Together, preclinical and clinical evidence indicate SST neurons are vulnerable to alcohol consumption in adults and may represent a potential therapeutic target for excessive alcohol consumption. However, limited work has explored the effects of alcohol exposure in adolescence on SST

neurons. In this study, we investigated the effects of adolescent binge drinking on PL cortical SST neurons, and how changes in PL SST neuronal properties may lead to compensatory changes on downstream pyramidal neurons within the PL cortex.

2. MATERIALS AND METHODS

2.1 Animals

All experiments were approved by the Pennsylvania State University Institutional Animal Care and Use Committee. Male and female SST-IRES-Cre (stock #013044, The Jackson Laboratory) and Ai9 (stock #007909, The Jackson Laboratory) mice were bred in-house. At post-natal day (PND) 21, SST-IRES-Cre:Ai9 mice were weaned into single housing and moved into a temperature- and humidity-controlled reverse light cycle room (lights off at 7:00 am) to acclimate for one week before experiments. Littermates were randomly assigned to either alcohol or control conditions as described below. Mice had *ad libitum* access to food and water, except during alcohol exposure.

2.2 Adolescent Drinking in the Dark (DID)

DID was conducted as previously published (Dao et al., 2021; Rhodes et al., 2005; Suresh Nair et al., 2022), at timepoints adapted for adolescence (Holstein et al., 2011; Dao et al., 2020) Mice received 20% (v/v) ethanol (EtOH; Koptec, Decon Labs, King of Prussia, PA) in tap water beginning 3 hr into the dark cycle, for 2 hr (i.e., 10:00 am to 12:00 pm) on three consecutive days. On the fourth day, EtOH was presented for 4 hr (i.e., 10:00 am to 2:00 pm), representing the "binge" day. Sipper tubes were weighed at the beginning and end of each drinking window. There were three days of abstinence between DID cycles. Mice underwent 4 cycles of DID, from postnatal day (PND) 28-52 or PND 30-54, during which control mice only had access to water but were otherwise treated identically (timeline in **Figure 1A**). The small stagger in the first exposure day was to allow time-locked electrophysiology from littermate cohorts of mice. Blood ethanol concentrations (BECs) were examined in a pilot cohort of SST-IRES-Cre:Ai9 mice to validate the adolescent DID consumption model (**Figure 1B-C**). Tail blood samples were taken 30 min after the final binge session. BECs were determined using an Analox. Additional cohorts of mice did not further undergoing tail blood sampling to minimize stress effects.

2.3 Electrophysiology

Whole-cell current-clamp electrophysiology was performed as previously described (Dao et al., 2021, 2020). Electrophysiology was conducted at two separate timepoints to assess either the short-term (24 hr post-DID) or long-term (30 day post-DID) effects of adolescent alcohol on PL neuronal intrinsic excitability. Mice were anesthetized with inhaled isoflurane and rapidly decapitated. Brains were rapidly removed and immediately placed in ice-cold, oxygenated *N*-methyl-*D*-glucamine (NMDG) cutting solution containing the following, in mM: 93 NMDG, 2.5 KCl, 1.2 NaH2PO4, 30 NaHCO3, 20 HEPES, 25 dextrose, 5 ascorbic acid, 2 thiourea, 3 sodium pyruvate, 10 MgSO4-7 H2O, 0.5 CaCl2-2 H2O, 306-310 mOsm, pH to 7.4 (Ting et al., 2018). Coronal slices 300 μm thick containing the PL cortex were prepared using a Compresstome vibrating microtome (Precisionary Instruments). Slices recovered in heated (31◦C), oxygenated NMDG buffer for a maximum of eight minutes before resting in heated, oxygenated artificial cerebrospinal fluid (aCSF) containing in mM: 124 NaCl, 4.0 KCl, 1.2 MgSO4-7 H2O, 2.0 CaCl2-2H2O, 1 NaH2PO4-H2O, 305-308 mOsm, for at least 1 hr before recording. For experiments, slices were moved to a submerged chamber where they were consistently perfused with heated, oxygenated aCSF at a rate of 2 mL/min.

SST neurons were identified based on the presence of the fluorescent tdTomato reporter using 565 nm LED excitation. Pyramidal neurons were identified based on morphology, membrane characteristics (resistance and capacitance), and action potential width as previously characterized (Dao et al., 2021). Recording electrodes (3-6 MΩ) were pulled from thin-walled borosilicate glass capillaries with a Narishige P-100 Puller. Electrodes were filled with a potassium gluconate-based intracellular recording solution, containing in mM: 135 potassium gluconic acid, 5 NaCl, 2 MgCl2-6H2O, 10 HEPES, 0.6 EGTA, 4 Na2ATP, and 0.4 Na2-GTP, 287-290 mOsm, pH 7.35. Properties measured to assess the intrinsic excitability of SST and pyramidal neurons in the PL cortex included resting membrane potential (RMP), rheobase, action potential threshold, and the number of action potentials fired during a voltage-current (VI) protocol. In the VI protocol, increasing steps of depolarizing current were injected into the neuron (0-200 pA, increasing by 10 pA per step, each step lasting 300 ms). Negative current steps were included as a control. Experiments were performed at each neuron's RMP and repeated holding the neurons at a common voltage of -70mV. Interspike interval (ISI) was calculated by measuring the

time between the peak of the first two action potentials of the 200 pA sweep during VI at RMP. Signals were digitized at 10 kHz and filtered at 4 kHz using a MultiClamp 700B amplifier. Recordings were analyzed using Clampfit 10.7 software (Molecular Devices, Sunnyvale, CA, United States). A maximum of 2 cells per cell type (i.e. 2 SST and 2 pyramidal) were recorded from each mouse.

2.4 Data analysis, statistics, and figure preparation

Data were analyzed in GraphPad Prism 7.0 (San Diego, CA, United States). A 2-way ANOVA (factors: sex, adolescent DID condition) was used for membrane properties including RMP, rheobase, action potential threshold, and ISI. A mixed effects ANOVA (factors: sex, adolescent DID condition, current injection step) was used for VI experiments. When a main effect of sex or an interaction between sex and DID condition was seen, males and females were further analyzed separately by 2-way ANOVA. Tukey post-hoc tests were used when appropriate. Data are presented as the mean and standard error of the mean. One cell was excluded from the ISI analysis from the male H2O group based on the ROUT test for outliers in GraphPad Prism. Excluding this cell did not impact the statistical outcome. For each cell type and timepoint, total alcohol consumption (g/kg) across the 4 cycles of adolescent DID were correlated with the number of action potentials elicited by a 200 pA current injection step at RMP. Control mice were included in correlations with g/kg consumed = 0. Each correlation was reported as Pearson's *r*.

3. RESULTS

3.1 Adolescent DID produces BECs above the threshold for binge drinking

An initial cohort of SST-IRES-Cre:Ai9 mice which underwent adolescent DID with tail blood collected 30 min after the final session. Adolescent DID exposed mice reached clinically significant BECs using our modified DID procedure (timeline **Figure 1A**, BECs **Figure 1B**). All DID mice drank to BECs exceeding the 80 mg/dL threshold for binge drinking. In addition, our DID procedure produces BECs comparable to previous studies using DID in adolescent C57 mice (Holstein et al., 2011; Wolstenholme et al., 2020) and matching our previous findings using adult mice (Dao et al., 2021). Due to the potential stress confound of tail blood sampling,

subsequent cohorts of mice did not undergo BEC analysis, but g/kg of alcohol consumed was recorded every session.

3.2 SST neuronal excitability was increased 24 hours after drinking

We sought to characterize immediate changes in the intrinsic excitability of PL SST neurons by performing electrophysiology 24 hr after the cessation of adolescent DID (**Figure 2**). RMP was not affected by sex or adolescent DID condition (representative traces in **Figure 2A-B,** RMP data in **Figure 2C;** $F_{sex}(1, 28) = 1.541$, $p = 0.2248$; $F_{DID}(1, 28) = 3.380$, $p = 0.0766$; $F_{sex \times DID}(1, 28) = 0.09798$; $p = 0.7566$). In rheobase experiments at RMP, we found a main effect of adolescent DID condition where SST neurons from alcohol exposed mice required significantly less current to fire an action potential (**Figure 2D;** $F_{DID}(1, 28) = 8.138$, $p = 0.0081$), though there was no main effect of sex or interaction between sex and adolescent DID condition ($F_{sex}(1, 28) = 0.5451$, $p = 0.4665$; $F_{sex \times DID}(1, 28) = 0.02432$; $p = 0.8772$). Action potential threshold was unaltered by adolescent DID condition (**Figure 2E;** $F_{sex}(1, 27) = 1.567$, $p = 0.2213$; $F_{DID}(1, 27) = 0.6358$, $p = 0.4322$; $F_{sex \times DID}(1, 27) = 0.2807$; $p = 0.6006$). In order to explore the potential underlying mechanisms of DID-induced changes in excitability, we also measured the interspike interval (ISI), or the interval between the first and second action potentials in the final step of the VI at RMP. Hyperpolarization-activated cyclic nucleotide (HCN) channels modulate properties related to neuronal excitability, including the ISI (Bohannon and Hablitz, 2018) and have previously been shown to be sensitive to adolescent alcohol in PL pyramidal neurons (Salling et al., 2018). However, the ISI in SST neurons was not altered by adolescent DID condition or sex (**Figure 2F;** $F_{sex}(1, 27) = 0.601$, $p = 0.4446$; $F_{DID}(1, 27) = 2.225$, $p = 0.1474$; $F_{sex \times DID}(1, 27) = 0.886$; $p = 0.3547$). We found a main effect of DID in the VI protocol at RMP (**Figure 2G;** females and males graphed separately in **Figure 2H-I**; mixed effects ANOVA with sex, alcohol exposure, and current injection as factors; $F_{DID}(1, 588) = 13.26$, $p = 0.0003$). There was an expected effect of current injection ($F_{current}(20, 588) = 36.25$, $p < 0.0001$). Higher current steps elicited more action potentials across all groups. There was no main effect of sex ($F_{sex}(1, 588) = 0.1753$; $p = 0.6756$). All interactions were not significant ($p > 0.05$).

We repeated the experiments holding the SST neurons at the common membrane potential of -70 mV. At -70 mV, the rheobase was unaltered by sex or adolescent DID condition (**Figure 2J;** $F_{sex}(1, 28) = 0.003726$,

p = 0.9518; $F_{DID}(1, 28) = 2.525$, p = 0.1233; $F_{sex\ x\ DID}(1, 28) = 0.1387$; p = 0.7124). Action potential threshold was similarly not affected by sex or adolescent DID while neurons were held at -70 mV (**Figure 2K;** $F_{sex}(1, 27)$ = 1.003, p = 0.3256; $F_{DID}(1, 27) = 0.1473$, p = 0.7041; $F_{sex\ x\ DID}(1, 27) = 0.8774$; p = 0.3572). In the VI protocol at -70 mV, we found significant main effects of sex (**Figure 2L**; mixed effects ANOVA with sex, alcohol exposure, and current injection as factors; $F_{sex}(1, 588) = 4.067$, p = 0.0442) and adolescent DID condition ($F_{DID}(1, 588)$ = 9.437, p =0.0022). We found an expected main effect of current injection ($F_{current}(20, 588) = 32.23$, $p < 0.0001$). Because of the main effect of sex, we further analyzed males and females separately using 2-way ANOVAs. In males, there was a main effect of adolescent DID (**Figure 2M**; F_{DID} (1, 252) = 7.003, p = 0.0087) and an expected main effect of current ($F_{current}(20, 252) = 16.35$, $p < 0.0001$). When held at -70mV, SST neurons from male mice which went through adolescent DID fired fewer action potentials overall compared to male mice which did not drink alcohol. There was no significant interaction between current and DID ($p > 0.05$). In females, there was only a significant effect of current injection (**Figure 2N**; $F_{current}(20, 336) = 15.66$, $p < 0.0001$) and no main effect of DID ($F_{DID}(20, 588) = 2.510$, p = 0.1141) or interaction ($p > 0.05$). Together, this suggested modest increases in SST neuronal excitability in the PL cortex following adolescent DID.

3.3 SST excitability remained increased 30 days after drinking

Next, we investigated how long SST neuronal hyperexcitability persisted after adolescent DID. In a separate cohort of mice, DID was repeated and then the mice were allowed to mature undisturbed from PND 54 to PND 84 before performing electrophysiology (**Figure 3**).

RMP was unaltered in SST neurons 30 days after adolescent DID (representative traces in **Figure 3A-B**, **Figure 3C** RMP data**;** $F_{sex}(1, 43) = 0.02353$, p = 0.8788; $F_{DID}(1, 43) = 0.03061$, p = 0.8619; $F_{sex\ x\ DID}(1, 43)$ = 1.298; p = 0.2609). Rheobase (**Figure 3D;** $F_{sex}(1, 43) = 0.3952$, p = 0.5329; $F_{DID}(1, 43) = 2.871$, p = 0.0974; $F_{sex\ x\ DID}(1, 43) = 0.04574$; p = 0.8317) and action potential threshold (**Figure 3E;** $F_{sex}(1, 43) = 1.691$, p = 0.2003; $F_{DID}(1, 43) = 1.361$, p = 0.2498; $F_{sex\ x\ DID}(1, 43) = 1.536$; p = 0.2220) were not changed as a function of sex or adolescent DID condition. There was no effect of adolescent DID condition or sex on the ISI (**Figure 3F**; $F_{sex}(1, 41) = 2.004$, p = 0.1644; $F_{DID}(1, 41) = 2.903$, p = 0.0960; $F_{sex\ x\ DID}(1, 43) = 1.098$; p = 0.3009). In the VI experiment at RMP, we found a significant interaction between current injection and DID condition (**Figure 3G**; mixed

effects ANOVA with sex, alcohol exposure, and current injection as factors; $F_{DID \times current}(20, 903) = 1.678$; $p = 0.0315$) as well as a significant main effect of sex $F_{sex}(1, 903) = 30.89$; $p < 0.0001$). All other interactions were not significant. Because we found a main effect of sex in our mixed effects analysis, we further analyzed the sexes separately as a 2-way ANOVA (factors: adolescent DID and current injection step). In males, we found significant main effects of current injection and adolescent DID condition (**Figure 3H;** $F_{current}(20, 441) = 31.25$, $p < 0.0001$; $F_{DID}(1, 441) = 43.39$, $p < 0.0001$; $F_{current \times DID}(20, 43) = 1.502$; $p = 0.0758$). In females, we found significant main effects of current and adolescent DID condition, with no significant interaction between adolescent DID and current injection (**Figure 3I;** $F_{current}(20, 462) = 24.02$, $p < 0.0001$; $F_{DID}(1, 462) = 46.84$, $p < 0.0001$; $F_{current \times DID}(20, 43) = 0.5528$; $p = 0.9426$).

We repeated these intrinsic excitability experiments holding the SST neurons at -70 mV. We found no main effect of sex or adolescent DID condition, or interaction between sex and adolescent DID condition, on rheobase at -70 mV (**Figure 3J;** $F_{sex}(1, 43) = 0.03137$, $p = .8602$; $F_{DID}(1, 43) = 2.659$, $p = 0.1103$; $F_{sex \times DID}(1, 43) = 0.2176$; $p = 0.6433$). Action potential threshold was also unaltered in SST neurons 30 days after adolescent DID (**Figure 3K;** $F_{sex}(1, 43) = 1.117$, $p = 0.2964$; $F_{DID}(1, 43) = 3.395$, $p = 0.0723$; $F_{sex \times DID}(1, 43) = 0.3319$; $p = 0.5675$). In the VI experiment conducted at -70 mV, we found a significant main effect of current (**Figure 3L;** mixed effects ANOVA with sex, alcohol exposure, and current injection as factors; $F_{current}(20, 903) = 67.44$; $p < 0.0001$) and a significant interaction between adolescent DID condition and sex ($F_{sex \times DID}(1, 903) = 8.528$; $p = 0.0036$). Because of this interaction, we then analyzed the sexes separately using a 2-way ANOVA. In males, there was a significant main effect of current (**Figure 3M**; $F_{current}(20, 441) = 28.68$; $p < 0.0001$) and of adolescent DID condition ($F_{DID}(1, 441) = 32.59$; $p < 0.0001$) but no significant interaction ($F_{current \times DID}(20, 462) = 1.452$; $p = 0.0940$). In females, there was a significant expected main effect of current (**Figure 3N;** $F_{current}(20, 462) = 39.82$; $p < 0.0001$) and a main effect of DID condition ($F_{DID}(1, 462) = 3.878$; $p = 0.0495$) but no significant current x DID interaction ($F_{current \times DID}(20, 462) = 0.3325$; $p = 0.9975$). Together, this suggested that adolescent DID-induced changes in SST function persisted well after the cessation of binge drinking and are likely permanent adaptations.

3.4 Pyramidal neuron excitability in reduced 24 hours after drinking

To determine if there are compensatory circuit changes after adolescent DID, we measured the intrinsic excitability of PL pyramidal neurons 24 hr after binge drinking ended (**Figure 4**). We found no effect of adolescent DID condition or sex on RMP (representative traces for rheobase and VI in **Figure 4A-B**, RMP data in **Figure 4C**; $F_{sex}(1, 30) < 0.0001$; $p = 0.9954$; $F_{DID}(1, 30) = 1.145$; $p = 0.2932$; $F_{sex \times DID}(1, 30) = 0.2332$; $p = 0.6327$). Rheobase was also unaltered by sex and adolescent DID condition (**Figure 4D**; $F_{sex}(1, 30) = 0.892$; $p = 0.3522$; $F_{DID}(1, 30) = 3.498$; $p = 0.0712$; $F_{sex \times DID}(1, 30) = 0.746$; $p = 0.3946$), as was action potential threshold (**Figure 4E**; $F_{sex}(1, 30) = 0.4251$; $p = 0.5194$; $F_{DID}(1, 30) = 0.05552$; $p = 0.8153$; $F_{sex \times DID}(1, 30) = 1.037$; $p = 0.3167$). However, there was a significant interaction between current injection step and DID condition during the VI protocol (**Figure 4F**; mixed effects ANOVA with sex, alcohol exposure, and current injection as factors; $F_{current \times DID}(20, 630) = 1.859$; $p = 0.0129$), as well as an interaction between sex and adolescent DID condition ($F_{sex \times DID}(1, 630) = 4.008$; $p = 0.0457$), on current-induced action potential firing. Because of the interaction between sex and adolescent DID, we analyzed the data separately by sex. A 2-way ANOVA revealed a main effect of current injection step and of adolescent DID condition in males (**Figure 4G**; $F_{current}(20, 294) = 7.633$; $p < 0.0001$, $F_{DID}(1, 294) = 31.63$; $p < 0.0001$; $F_{current \times DID}(20, 294) = 1.378$; $p = 0.1312$). Similarly, there were significant main effects of current injection and adolescent DID condition in pyramidal neurons from females (**Figure 4H**; $F_{current}(20, 336) = 14.93$; $p < 0.0001$, $F_{DID}(1, 336) = 16.21$; $p < 0.0001$; $F_{current \times DID}(20, 336) = 0.5181$; $p = 0.9587$). In both sexes, PL pyramidal neurons showed reduced excitability following adolescent DID.

We then assessed the excitability of pyramidal neurons while holding the neurons at a common voltage of -70 mV. There was no effect of sex or adolescent DID condition on rheobase in neurons held at -70 mV (**Figure 4I**; $F_{sex}(1, 30) = 0.06683$; $p = 0.7978$, $F_{DID}(1, 30) = 0.1914$; $p = 0.6649$; $F_{sex \times DID}(1, 30) = 1.880$; $p = 0.1804$). Neither sex nor adolescent DID condition altered action potential threshold when the neurons were held at -70mV (**Figure 4J**; $F_{sex}(1, 30) = 0.3422$; $p = 0.5630$, $F_{DID}(1, 30) = 0.3345$; $p = 0.5674$; $F_{sex \times DID}(1, 30) = 0.005682$; $p = 0.9404$). We found significant main effects of current injection, sex, and adolescent DID on current-induced action potential firing when pyramidal neurons were held at -70mV (**Figure 4K**; mixed effects ANOVA with sex, alcohol exposure, and current injection as factors; $F_{current}(20, 630) = 10.57$; $p < 0.0001$; $F_{sex}(1, 630) = 6.202$; $p = 0.0130$, $F_{DID}(1, 630) = 18.26$; $p < 0.0001$). All interactions were not significant ($p > 0.05$). Because we found a main effect of sex, we analyzed the data from males and females separately using a 2-way ANOVA. In males,

there was an expected main effect of current injection (**Figure 4L**; $F_{current}(20, 294) = 5.701$; $p < 0.0001$) and a main effect of adolescent DID ($F_{DID}(1, 294) = 6.874$; $p = 0.0092$), but no interaction between current and DID ($F_{current\ x\ DID}(20, 294) = 0.3311$; $p = 0.9974$). In females, we found similar effects of current injection (**Figure 4M**; $F_{current}(20, 336) = 4.724$; $p < 0.0001$) and adolescent DID ($F_{DID}(1, 336) = 12.86$; $p = 0.0004$) with no interaction ($F_{current\ x\ DID}(20, 336) = 0.5633$; $p = 0.9359$). Together these results indicate an immediate reduction on pyramidal neuron excitability in both males and females after adolescent binge drinking.

3.5 Pyramidal neuron excitability 30 days after drinking

We next measured persistent changes in pyramidal neuron intrinsic excitability 30 days after adolescent DID concluded (**Figure 5**). Neither adolescent DID condition nor sex altered RMP of pyramidal neurons (representative traces for rheobase and VI in **Figure 5A-B,** RMP data in **Figure 5C;** $F_{sex}(1, 39) = 0.7440$; $p = 0.39$; $F_{DID}(1, 39) = 1.408$; $p = 0.24$; $F_{sex\ x\ DID}(1, 39) = 0.04382$; $p = 0.84$). Rheobase did not change as a function of sex or adolescent DID condition (**Figure 5D;** $F_{sex}(1, 39) = 0.01389$; $p = 0.91$; $F_{DID}(1, 39) = 1.477$; $p = 0.23$; $F_{sex\ x\ DID}(1, 39) = 0.004107$; $p = 0.95$). Action potential was also unaltered (**Figure 5E;** $F_{sex}(1, 39) = 0.4450$; $p = 0.51$; $F_{DID}(1, 39) = 0.3607$; $p = 0.55$; $F_{sex\ x\ DID}(1, 39) = 0.01289$; $p = 0.91$). In the VI protocol at RMP, we found an expected main effect of current (**Figure 5F;** mixed effects ANOVA with sex, alcohol exposure, and current injection as factors; $F_{current}(20, 819) = 18.00$; $p < 0.0001$) but no effect of sex ($F_{sex}(1, 819) = 2.772$; $p = 0.0963$) or adolescent DID condition ($F_{DID}(1, 819) = 1.500$; $p = 0.2210$). There was not a significant interaction between sex and adolescent DID condition ($F_{sex\ x\ DID}(1, 819) = 3.355$; $p = 0.0674$); however, due to the strong sex-dependent effects throughout the circuit and during the 24 hr timepoint we then analyzed the data separately by sex. In males, there was an expected effect of current injection (**Figure 4G;** $F_{current}(20, 336) = 7.645$; $p < 0.0001$) but no effect of adolescent DID condition ($F_{DID}(1, 336) = 0.1313$; $p = 0.7173$) and no interaction ($F_{current\ x\ DID}(20, 336) = 0.01189$; $p > 0.9999$). However, in females, there were significant main effects of current (**Figure 4H;** $F_{current}(20, 483) = 10.46$; $p > 0.0001$) and adolescent DID condition ($F_{DID}(1, 483) = 6.525$; $p = 0.0109$), but no interaction ($F_{current}$ x DID$(20, 483) = 0.5006$; $p = 0.9664$).

We repeated the experiments holding the neurons at the common membrane potential of -70 mV. At -70 mV, there was no effect of adolescent DID condition or sex on rheobase (**Figure 5I;** $F_{sex}(1, 39) = 0.1949$; $p =$

0.6613; $F_{DID}(1, 39) = 0.08767$; $p = 0.7687$; $F_{sex \times DID}(1, 39) = 0.5122$; $p = 0.4784$) or action potential threshold (**Figure 5J;** $F_{sex}(1, 39) = 0.09984$; $p = 0.7537$; $F_{DID}(1, 39) = 0.9601$; $p = 0.3332$; $F_{sex \times DID}(1, 39) = 0.002495$; $p = 0.9604$). In the VI protocol at -70 mV, we found an expected main effect of current (**Figure 5K;** mixed effects ANOVA with sex, alcohol exposure, and current injection as factors; $F_{current}(20, 819) = 16.79$; $p < 0.0001$). However, there was no effect of sex ($F_{sex}(1, 819) = 1.824$; $p = 0.1773$) or adolescent DID condition ($F_{DID}(1, 819) = 0.1891$; $p = 0.6638$). As above, we further analyzed the sexes separately as a 2-way ANOVA due to the sex differences seen at the 24 hr timepoint and throughout the circuit. We found an expected main effect of current injection, but no effect of adolescent DID in males (**Figure 5L;** $F_{current}(20, 336) = 6.758$; $p < 0.0001$; $F_{DID}(1, 336) = 0.5322$; $p = 0.4662$) and in females (**Figure 5M;** $F_{current}(20, 483) = 10.29$; $p < 0.0001$; $F_{DID}(1, 483) = 3.343$; $p = 0.0681$). Together, these results suggest that PL pyramidal neurons in layer II/III may rebound towards hyperexcitability 30 days after adolescent DID, potentially to compensate for permanent increases in GABAergic signaling arising from overactive SST neurons.

3.6 Relationship between altered excitability and alcohol consumed during the binge paradigm

We next sought to understand how individual variability in alcohol consumption drove overall changes in cortical excitability. As the most prominent changes were identified in the VI protocol, we correlated the number of action potentials fired during the last step of the VI in SST neurons and pyramidal neurons with the g/kg alcohol consumed throughout the 4 week DID exposure (**Figure 6**). Total alcohol consumption was not correlated with SST action potential firing 24 hr after DID in males (**Figure 6A**; $r(12) = -0.125$, $p = 0.669$) or females (**Figure 6B**; $r(16) = -0.044$, $p = 0.863$). In SST neurons from adult male mice (30 days after the cessation of DID), total alcohol consumption across the adolescent DID paradigm was significantly correlated with the number of action potentials fired during the last step of VI (**Figure 6C**; $r(21) = 0.464$, $p = 0.026$). However, total drinking was not correlated with action potential firing in adult females (**Figure 6D;** $r(22) = 0.137$, $p = 0.523$). In pyramidal neurons recorded 24 hr after binge drinking, total alcohol consumption during the 4 weeks of adolescent DID was not significantly correlated with action potentials fired in males (**Figure 6E**; $r(14) = -0.421$; $p = 0.105$) or females (**Figure 6F;** $r(16) = -0.282$, $p = 0.256$). In adult mice, total alcohol drinking during adolescence was not correlated with current-induced action potential firing in males (**Figure 6G**; $r(16)$

= -0.042, p = 0.870) or females (**Figure 6H;** $r(23)$ = 0.250, p = 0.229). Together, these results indicate that alcohol consumption in adolescence is correlated with SST neuronal dysfunction in adult male mice.

4. DISCUSSION

Our work suggests that adolescent binge alcohol consumption via a modified DID model leads to modest but persistent alterations in cortical SST excitability. We also provide preliminary evidence that this effect is not driven by HCN-channel alterations, as evident by no change in the action potential firing rate as measured by the ISI of SST neurons. These general changes are consistent with a broad literature suggesting chronic adaptations in the cortex following adolescent models of alcohol exposure. Chronic ethanol administration induced sex-specific changes in the excitability of PL Martinotti neurons in adult rats, an effect mediated by differences in HCN channel function (Hughes et al., 2020). Changes in HCN channel function have also been reported in PL pyramidal neurons following adolescent alcohol exposure, leading to PL layer V pyramidal neuron hyperexcitability (Salling et al., 2018). However, we did not find changes in the ISI in SST neurons, suggesting that other mechanisms may also contribute to SST neuronal hyperexcitability. It is possible that HCN channel vulnerability is limited to deeper layers of the PL cortex. Future experiments should more explicitly explore HCN channel expression and function on SST neurons following adolescent alcohol.

As noted above, some studies have found persistent alterations in PL layer V pyramidal neuronal excitability after adolescent alcohol (Salling et al., 2018). In addition, intermittent exposure to alcohol during adolescence prevented the typical development of a tonic GABAergic current onto PL pyramidal neurons only in layer V (Centanni et al., 2017). Hyperexcitability may be most prominent in V pyramidal neurons, as others have shown that adolescent alcohol does not alter the intrinsic excitability of layer II pyramidal neurons in the short- or long-term in rats (Galaj et al., 2020). In our current study, we targeted layer II/III neurons in the PL cortex and found general increases in excitability weeks after the cessation of alcohol exposure. Galaj and colleagues used both a different species (rats) and a differing model of ethanol exposure (chronic intermittent ethanol exposure), highlighting the need for precise comparisons across differing models of alcohol exposure, and that models may not generalize across each other in their long-term effects (Crowley et al., 2019). Together, these

findings all suggest that the consequences of alcohol exposure are age-dependent and may be layer-specific in the PL cortex, and can persist well into adulthood.

We have shown here that adolescent binge drinking causes persistent alterations in PL SST neuronal excitability; however, corresponding changes in SST peptide release following binge drinking remain under investigation. Although limited work has assessed changes in SST peptide release or expression in substance use disorders, SST represents a potential therapeutic target for a variety of neuropsychiatric illnesses (Brockway and Crowley, 2020). Future experiments should investigate changes in SST peptide release throughout development and following alcohol exposure using both optogenetic techniques (Dao et al., 2019), *in vivo* recording (Brockway et al., 2022, preprint), and novel biosensors (Wang et al., 2022, preprint; Xiong et al., 2021, preprint).

PL SST neurons have been implicated in anxiety-like behavior (Soumier and Sibille, 2014). Studies assessing changes in anxiety-like behavior following adolescent alcohol have found mixed results, with some showing increases in anxiety-like behavior after adolescent drinking (Lee et al., 2017; Varlinskaya et al., 2020) and others showing no change (Amodeo et al., 2018). While the current study did not explore the behavioral ramifications of long-term SST excitability, the literature has long suggested a broad role for these neurons in fear learning (Cummings and Clem, 2020), threat response (Joffe et al., 2022), and alcohol use itself (Dao et al., 2021), and we have recently shown their active engagement during exploratory behaviors (Brockway et al., 2022, preprint). Therefore, the consequences of a lifelong increase in SST function may be catastrophic to the individual brain.

4. CONCLUSIONS

Here, we provide increased validation for adolescent binge drinking as a clinically relevant model of binge ethanol consumption. We demonstrate that binge drinking during a broad definition of adolescence leads to increased excitability of PL SST neurons, which persists well into adulthood.

5. FUNDING

This work was funded by the National Institutes of Health (R01 AA 209403, R21 AA028088, and P50 AA017823 to NAC; F31AA0304550-01 and GM108563 T32 training fellowship to ARS).

6. REFERENCES

Amodeo, L.R., Wills, D.N., Sanchez-Alavez, M., Nguyen, W., Conti, B., Ehlers, C.L., 2018. Intermittent voluntary ethanol consumption combined with ethanol vapor exposure during adolescence increases drinking and alters other behaviors in adulthood in female and male rats. Alcohol 73, 57–66. https://doi.org/10.1016/J.ALCOHOL.2018.04.003

Bohannon, A.S., Hablitz, J.J., 2018. Developmental Changes in HCN Channel Modulation of Neocortical Layer 1 Interneurons. Frontiers in Cellular Neuroscience 12. https://doi.org/10.3389/fncel.2018.00020

Brockway, D.F., Crowley, N.A., 2020. Turning the 'Tides on Neuropsychiatric Diseases: The Role of Peptides in the Prefrontal Cortex. Frontiers in Behavioral Neuroscience 14, 182. https://doi.org/10.3389/FNBEH.2020.588400/BIBTEX

Brockway, D.F., Moyer, J.B., Aloimonos, C.M., Clarity, T., Griffith, K.R., Smith, G.C., Dao, N.C., Hossain, M.S., Drew, P.J., Gordon, J.A., Kupferschmidt, D.A., Crowley, N.A., 2022. Somatostatin peptide signaling dampens cortical circuits and promotes exploratory behavior. bioRxiv .

Centanni, S.W., Burnett, E.J., Trantham-Davidson, H., Chandler, L.J., 2017. Loss of δ–GABAA receptor-mediated tonic currents in the adult prelimbic cortex following adolescent alcohol exposure. Addiction biology 22, 616. https://doi.org/10.1111/ADB.12353

Crowley, N.A., Dao, N.C., Magee, S.N., Bourcier, A.J., Lowery-Gionta, E.G., 2019. Animal models of alcohol use disorder and the brain: From casual drinking to dependence. Translational Issues in Psychological Science 5, 222–242. https://doi.org/10.1037/TPS0000198

Cummings, K.A., Clem, R.L., 2020. Prefrontal somatostatin interneurons encode fear memory. Nat Neurosci 23, 61. https://doi.org/10.1038/S41593-019-0552-7

Dao, N.C., Brockway, D.F., Crowley, N.A., 2019. In Vitro Optogenetic Characterization of Neuropeptide Release from Prefrontal Cortical Somatostatin Neurons. Neuroscience 419, 1–4. https://doi.org/10.1016/J.NEUROSCIENCE.2019.08.014

Dao, N.C., Brockway, D.F., Suresh Nair, M., Sicher, A.R., Crowley, N.A., 2021. Somatostatin neurons control an alcohol binge drinking prelimbic microcircuit in mice. Neuropsychopharmacology 46, 1906–1917. https://doi.org/10.1038/S41386-021-01050-1

Dao, N.C., Suresh Nair, M., Magee, S.N., Moyer, J.B., Sendao, V., Brockway, D.F., Crowley, N.A., 2020. Forced Abstinence From Alcohol Induces Sex-Specific Depression-Like Behavioral and Neural Adaptations in Somatostatin Neurons in Cortical and Amygdalar Regions. Frontiers in Behavioral Neuroscience 14, 86. https://doi.org/10.3389/FNBEH.2020.00086/BIBTEX

Donovan, J.E., 2009. Estimated blood alcohol concentrations for child and adolescent drinking and their implications for screening instruments. Pediatrics 123. https://doi.org/10.1542/PEDS.2008-0027

Du, X., Serena, K., Hwang, W., Grech, A.M., Wu, Y.W.C., Schroeder, A., Hill, R.A., 2018. Prefrontal cortical parvalbumin and somatostatin expression and cell density increase during adolescence and are modified by BDNF and sex. Molecular and Cellular Neuroscience 88, 177–188. https://doi.org/10.1016/J.MCN.2018.02.001

Galaj, E., Guo, C., Huang, D., Ranaldi, R., Ma, Y.Y., 2020. Contrasting effects of adolescent and early-adult ethanol exposure on prelimbic cortical pyramidal neurons. Drug and Alcohol Dependence 216, 108309. https://doi.org/10.1016/J.DRUGALCDEP.2020.108309

Holstein, S.E., Spanos, M., Hodge, C.W., 2011. Adolescent C57BL/6J Mice Show Elevated Alcohol Intake, but Reduced Taste Aversion, as Compared to Adult Mice: A Potential Behavioral Mechanism for Binge Drinking. Alcoholism: Clinical and Experimental Research 35, 1842–1851. https://doi.org/10.1111/J.1530-0277.2011.01528.X

Hughes, B.A., Crofton, E.J., O'Buckley, T.K., Herman, M.A., Morrow, A.L., 2020. Chronic ethanol exposure alters prelimbic prefrontal cortical Fast-Spiking and Martinotti interneuron function with differential sex specificity in rat brain. Neuropharmacology 162, 107805. https://doi.org/10.1016/J.NEUROPHARM.2019.107805

Joffe, M.E., Maksymetz, J., Luschinger, J.R., Dogra, S., Ferranti, A.S., Luessen, D.J., Gallinger, I.M., Xiang, Z., Branthwaite, H., Melugin, P.R., Williford, K.M., Centanni, S.W., Shields, B.C., Lindsley, C.W., Calipari, E.S., Siciliano, C.A., Niswender, C.M., Tadross, M.R., Winder, D.G., Conn, P.J., 2022. Acute restraint stress redirects prefrontal cortex circuit function through mGlu5 receptor plasticity on somatostatin-expressing interneurons. Neuron 110, 1068-1083.e5. https://doi.org/10.1016/J.NEURON.2021.12.027

Joffe, M.E., Winder, D.G., Conn, P.J., 2020. Contrasting sex-dependent adaptations to synaptic physiology and membrane properties of prefrontal cortex interneuron subtypes in a mouse model of binge drinking. Neuropharmacology 178, 108126. https://doi.org/10.1016/j.neuropharm.2020.108126

Koppensteiner, P., von Itter, R., Melani, R., Galvin, C., Lee, F.S., Ninan, I., 2019. Diminished fear extinction in adolescents is associated with an altered somatostatin interneuron-mediated inhibition in the infralimbic cortex. Biol Psychiatry 86, 682. https://doi.org/10.1016/J.BIOPSYCH.2019.04.035

Lawson, K., Scarlata, M.J., Cho, W.C., Mangan, C., Petersen, D., Thompson, H.M., Ehnstrom, S., Mousley, A.L., Bezek, J.L., Bergstrom, H.C., 2022. Adolescence alcohol exposure impairs fear extinction and alters medial prefrontal cortex plasticity. Neuropharmacology 211, 109048. https://doi.org/10.1016/J.NEUROPHARM.2022.109048

Lee, K.M., Coehlo, M.A., Solton, N.R., Szumlinski, K.K., 2017. Negative affect and excessive alcohol intake incubate during protracted withdrawal from binge-drinking in adolescent, but not adult, mice. Frontiers in Psychology 8, 1128. https://doi.org/10.3389/FPSYG.2017.01128/BIBTEX

NIAAA, 2021. Underage Drinking | National Institute on Alcohol Abuse and Alcoholism (NIAAA) [WWW Document]. URL https://www.niaaa.nih.gov/publications/brochures-and-fact-sheets/underage-drinking (accessed 7.31.22).

Ochi, R., Ueno, F., Sakuma, M., Tani, H., Tsugawa, S., Graff-Guerrero, A., Uchida, H., Mimura, M., Oshima, S., Matsushita, S., Nakajima, S., 2022. Patterns of functional connectivity alterations induced by alcohol reflect somatostatin interneuron expression in the human cerebral cortex. Scientific Reports 2022 12:1 12, 1–9. https://doi.org/10.1038/s41598-022-12035-5

Pan, G., Yang, J.M., Hu, X.Y., Li, X.M., 2016. Postnatal development of the electrophysiological properties of somatostatin interneurons in the anterior cingulate cortex of mice. Scientific Reports 2016 6:1 6, 1–12. https://doi.org/10.1038/srep28137

Rhodes, J.S., Best, K., Belknap, J.K., Finn, D.A., Crabbe, J.C., 2005. Evaluation of a simple model of ethanol drinking to intoxication in C57BL/6J mice. Physiology & Behavior 84, 53–63. https://doi.org/10.1016/j.physbeh.2004.10.007

Salling, M.C., Skelly, M.J., Avegno, E., Regan, S., Zeric, T., Nichols, E., Harrison, N.L., 2018. Alcohol Consumption during Adolescence in a Mouse Model of Binge Drinking Alters the Intrinsic Excitability and Function of the Prefrontal Cortex through a Reduction in the Hyperpolarization-

Activated Cation Current. Journal of Neuroscience 38, 6207–6222. https://doi.org/10.1523/JNEUROSCI.0550-18.2018

Sicher, A.R., Duerr, A., Starnes, W.D., Crowley, N.A., 2022. Adolescent Alcohol and Stress Exposure Rewires Key Cortical Neurocircuitry. Frontiers in Neuroscience 0, 623. https://doi.org/10.3389/FNINS.2022.896880

Soumier, A., Sibille, E., 2014. Opposing Effects of Acute versus Chronic Blockade of Frontal Cortex Somatostatin-Positive Inhibitory Neurons on Behavioral Emotionality in Mice. Neuropsychopharmacology 2014 39:9 39, 2252–2262. https://doi.org/10.1038/npp.2014.76

Suresh Nair, M., Dao, N.C., Lopez Melean, D., Griffith, K.R., Starnes, W.D., Moyer, J.B., Sicher, A.R., Brockway, D.F., Meeks, K.D., Crowley, N.A., 2022. Somatostatin neurons in the bed nucleus of the stria terminalis play a sex-dependent role in binge Drinking. Brain Research Bulletin 186, 38–46. https://doi.org/10.1016/J.BRAINRESBULL.2022.05.010

Ting, J.T., Lee, B.R., Chong, P., Soler-Llavina, G., Cobbs, C., Koch, C., Zeng, H., Lein, E., 2018. Preparation of Acute Brain Slices Using an Optimized N-Methyl-D-glucamine Protective Recovery Method. Journal of Visualized Experiments. https://doi.org/10.3791/53825

Varlinskaya, E.I., Hosová, D., Towner, T., Werner, D.F., Spear, L.P., 2020. Effects of chronic intermittent ethanol exposure during early and late adolescence on anxiety-like behaviors and behavioral flexibility in adulthood. Behavioural Brain Research 378, 112292. https://doi.org/10.1016/J.BBR.2019.112292

Wang, H., Qian, T., Zhao, Y., Zhuo, Y., Wu, C., Osakada, T., Chen, P., Ren, H., Yan, Y., Geng, L., Fu, S., Mei, L., Li, G., Wu, L., Jiang, Y., Qian, W., Peng, W., Xu, M., Hu, J., Chen, L., Tang, C., Lin, D., Zhou, J.-N., Li, Y., 2022. A toolkit of highly selective and sensitive genetically encoded neuropeptide sensors. bioRxiv.

Wolstenholme, J.T., Younis, R.M., Toma, W., Damaj, M.I., 2020. Adolescent low-dose ethanol drinking in the dark increases ethanol intake later in life in C57BL/6J, but not DBA/2J mice. Alcohol 89, 85–91. https://doi.org/10.1016/J.ALCOHOL.2020.08.005

Xiong, H., Lacin, E., Ouyang, H., Naik, A., Xu, X., Xie, C., Youn, J., Kumar, K., Kern, T., Aisenberg, E., Kircher, D., Li, X., Zasadzinski, J.A., Mateo, C., Kleinfeld, D., Hrabetova, S., Slesinger, P.A., Qin, Z., 2021. Probing neuropeptide volume transmission in vivo by a novel all-optical approach. bioRxiv 2021.09.10.459853. https://doi.org/10.1101/2021.09.10.459853

Xu, X., Roby, K.D., Callaway, E.M., 2010. Immunochemical characterization of inhibitory mouse cortical neurons: Three chemically distinct classes of inhibitory cells. J Comp Neurol 518, 389. https://doi.org/10.1002/CNE.22229

FIGURE 1

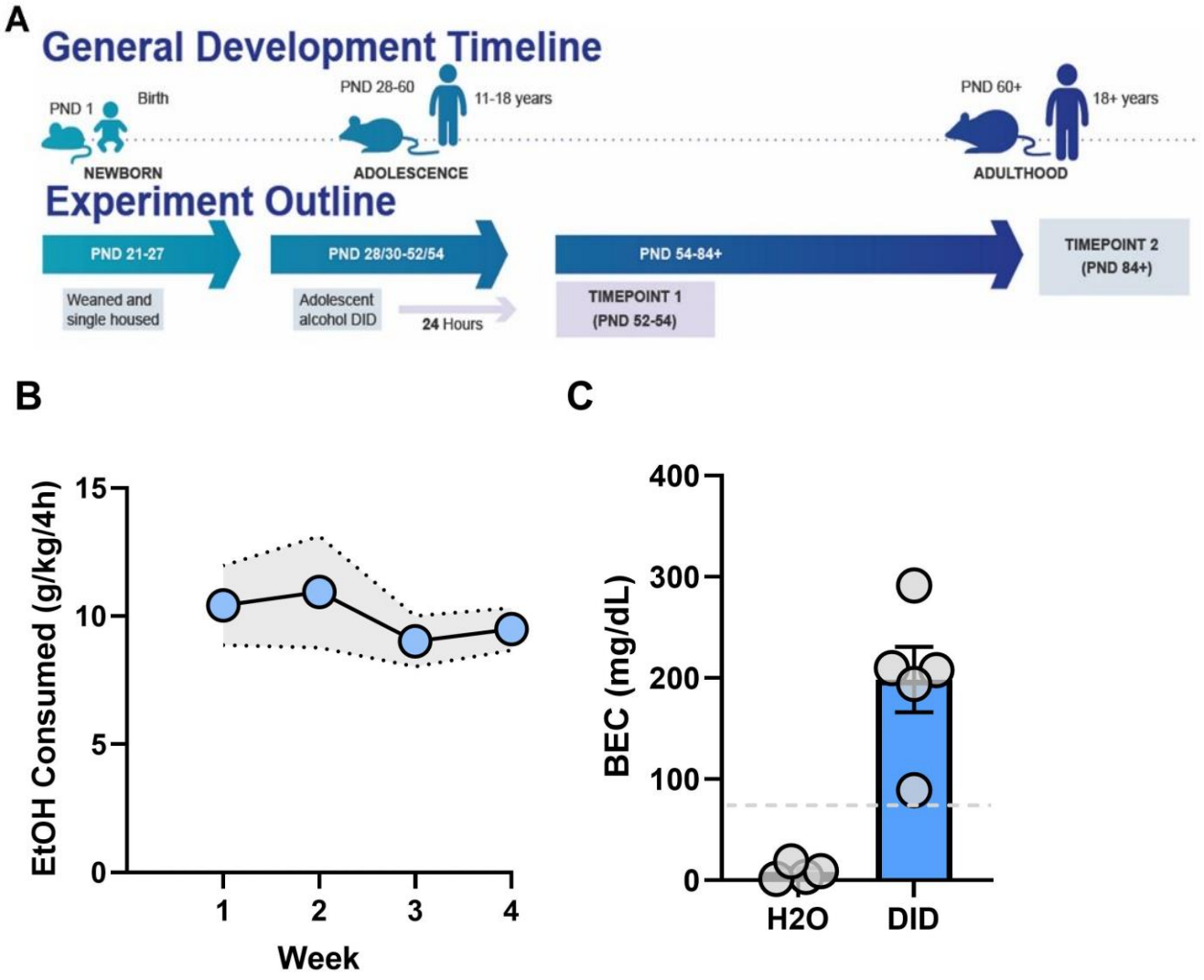

Figure 1 Overall experimental timeline. (A) Adolescent development of mice versus humans. Alcohol is administered during PND 28/30-52/54, corresponding to a broad range of adolescence in humans. **(B)** Average g/kg of ethanol consumed on the binge day for all 4 weeks in a pilot cohort of mice. Shaded areas represent SEM. **(C)** Blood ethanol concentrations above the 80 mg / dL levels corresponding to a 'binge' episode.

FIGURE 2

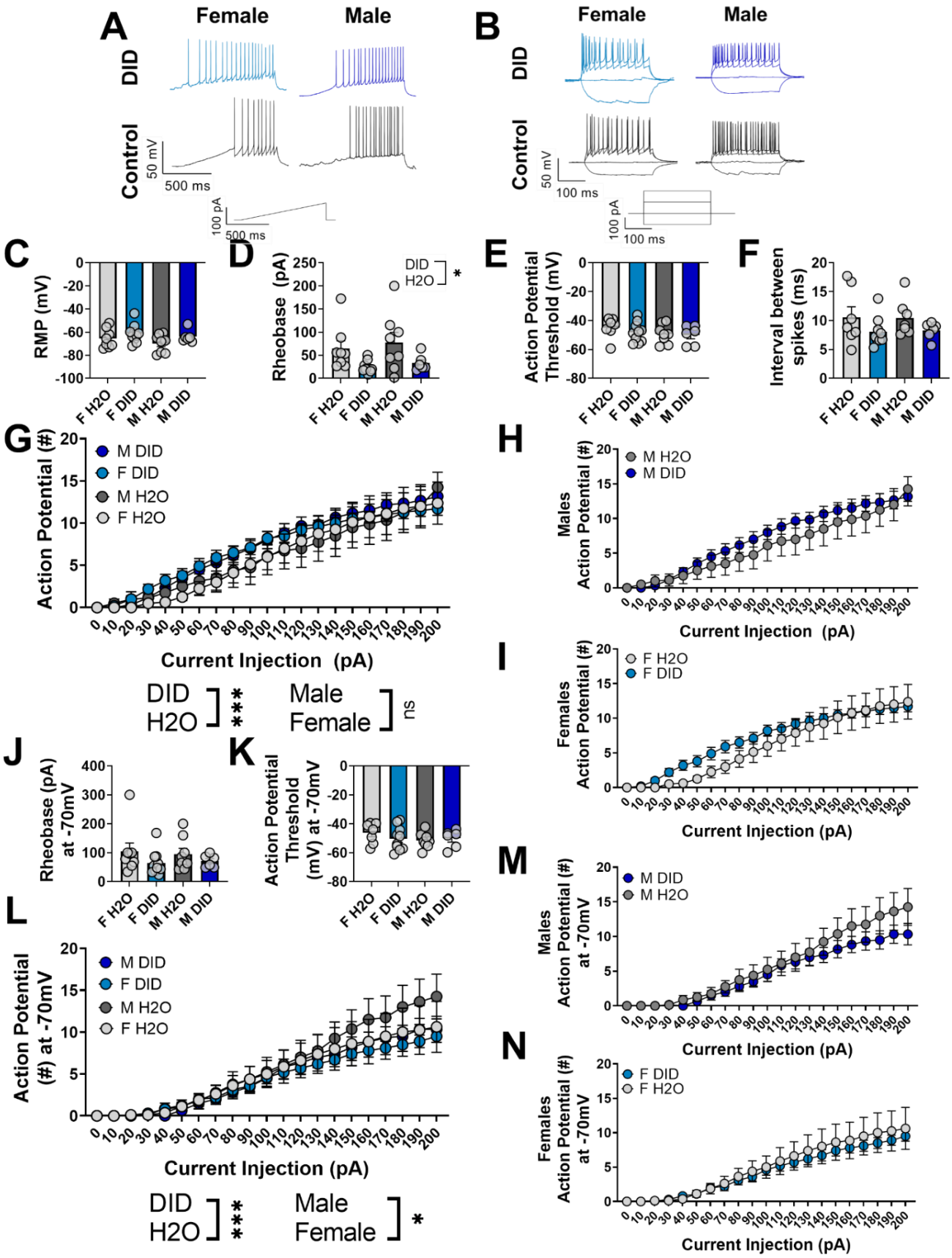

Figure 2. SST neurons are hyperexcitable 24 hr after adolescent DID. (A-B) Representative traces for rheobase and VI at RMP. (C-D) RMP is not altered by adolescent DID or sex, although SST neurons from mice which went through DID require less current to elicit an action potential. (E-F) Action potential threshold and interspike interval are not altered by adolescent DID or sex. (G) SST neurons from mice which drank alcohol during adolescence fired more action potentials compared to SST neurons from mice which did not drink during adolescence. (H-I) Data from (G), separated by sex for visualization. (J-K) Membrane properties of SST neurons were unaltered by sex or adolescent DID condition when neurons were held at -70mV. (L) There was a main effect of adolescent DID condition and of sex on the number of action potentials fired when SST neurons were held at -70mV. (M-N) Data from (L) split by sex for visualization. For panels A-L, n = 6 cells from 3 mice (M DID), 10 cells from 5 mice (F DID), 8 cells from 4 mice (M H2O), and 8 cells from 5 mice (F H2O).

FIGURE 3

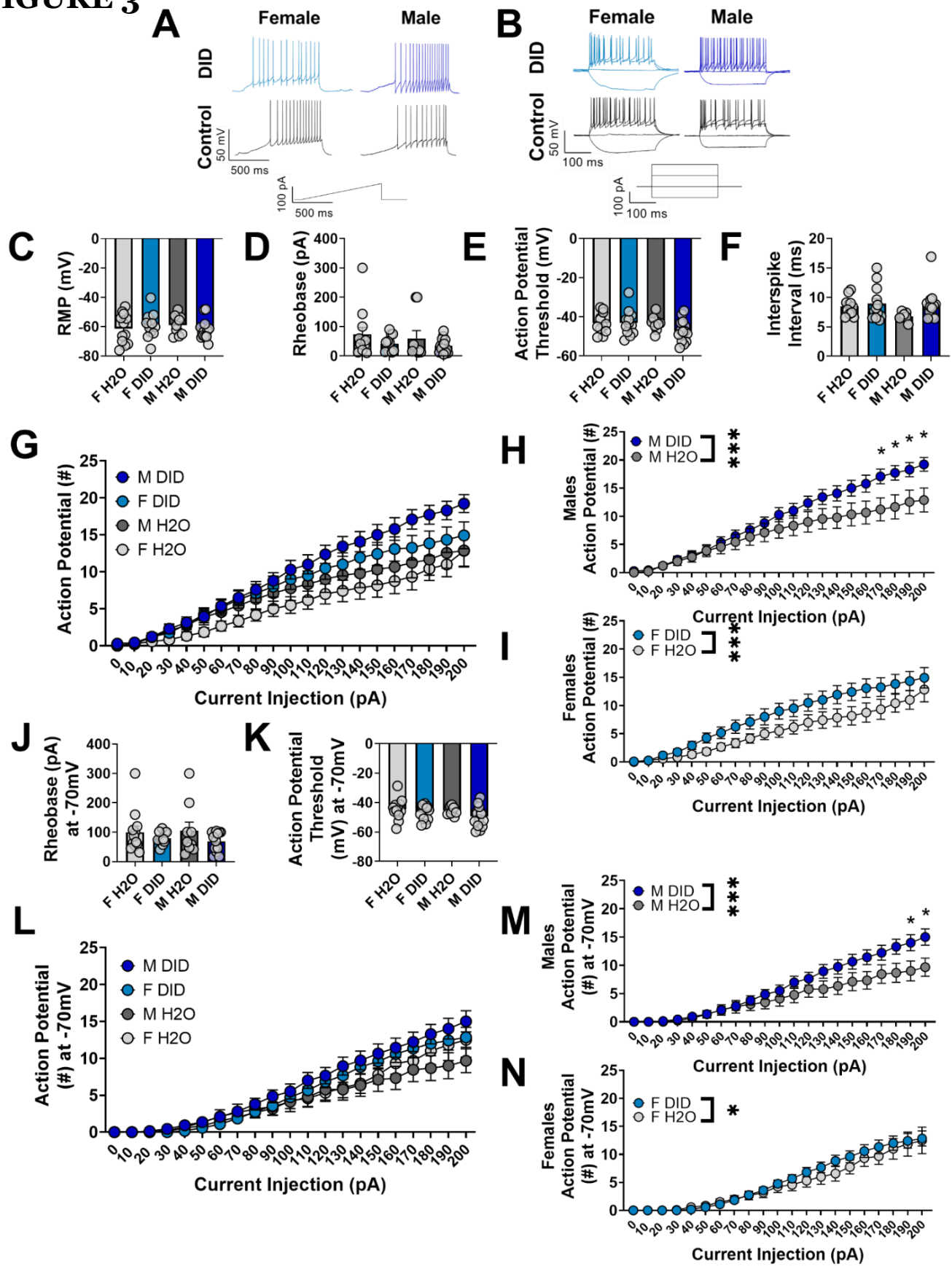

Figure 3. SST neurons remain hyperexcitable 30 days after cessation of adolescent DID. (A-B) Representative traces for rheobase and VI recordings. (C-F) Membrane properties and interspike interval of SST neurons were not altered as a function of adolescent DID or sex. (G) At RMP, we found a significant interaction of current injection step and adolescent DID condition, and a main effect of sex on current-induced action potential firing. (H-I) When the data from (G) at RMP were analyzed separately based on sex, there was a significant main effect of adolescent DID in both males and females. (J-K) Membrane properties of SST neurons were not altered when neurons were held at -70mV. (L) When held at -70mV, there was a significant interaction between sex and adolescent DID, as well as a main effect of current injection on current-induced action potential firing. (M-N) Data from (L) graphed separately by sex. When analyzed separately, there was a main effect of adolescent DID on the number of action potentials fired in both males and females. For panels A-L, n = 14 cells from 7 mice (M DID), 12 cells from 6 mice (F DID), 9 cells from 5 mice (M H2O), and 12 cells from 6 mice (F H2O). * indicates $p < 0.05$, *** indicates $p < 0.0001$. Main effects of adolescent DID or sex are indicated with brackets between group labels; significant differences in current-induced firing are indicated with * over specific current steps.

FIGURE 4

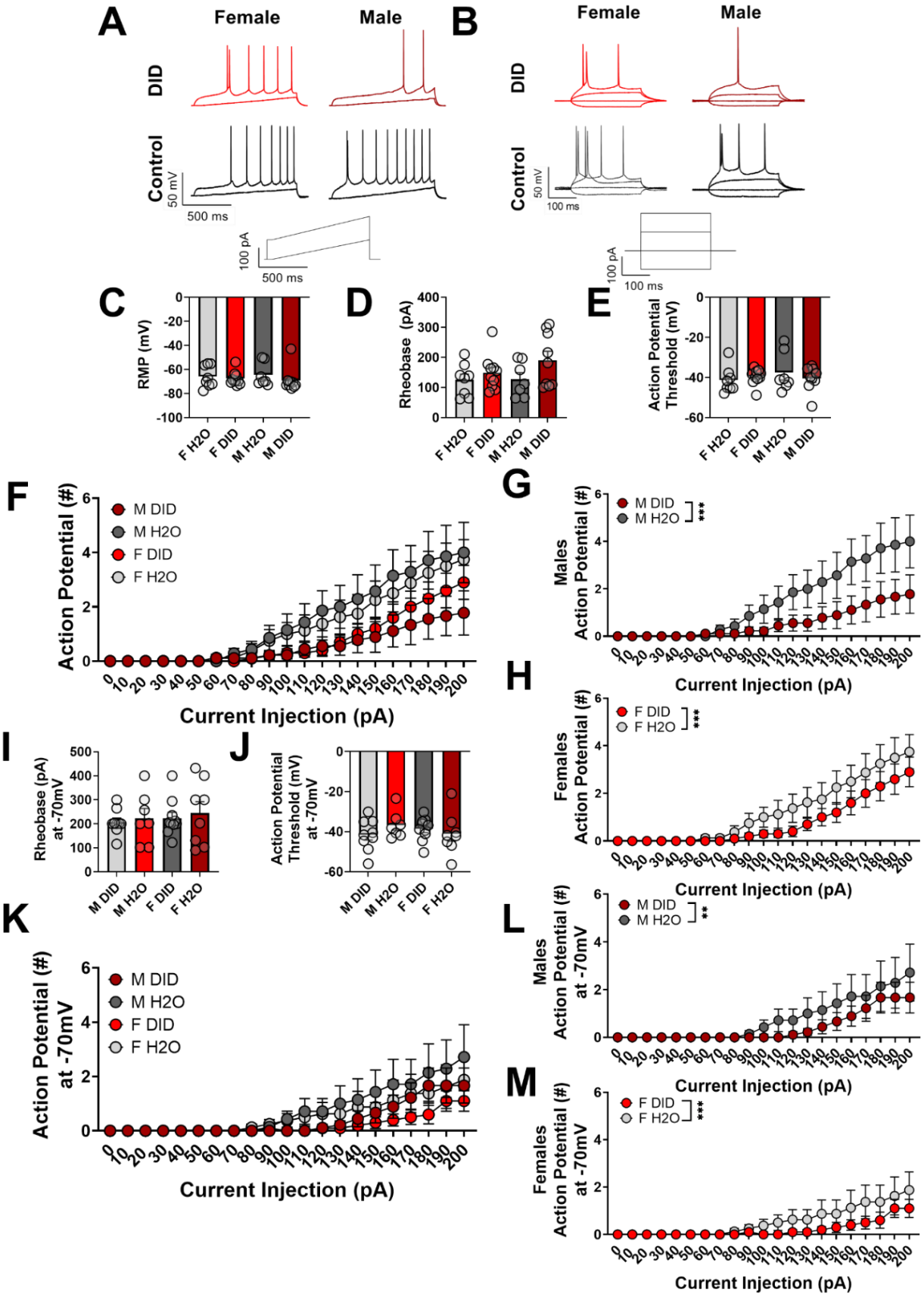

Figure 4. Pyramidal neurons are hypoexcitable 24 hr after adolescent DID. (A-B) Representative traces for rheobase and VI experiments in pyramidal neurons 24 hr after binge drinking. (C-E) There were no significant differences in RMP, rheobase, or action potential threshold as a function of adolescent DID or sex. (F) At RMP, we found a significant interaction between sex and adolescent DID as well as an expected main effect of current on current-induced action potential firing. (G-H) Data from (F) graphed separately by sex. When analyzed separately by sex, adolescent DID reduced action potential firing in both males and females. (I-J) Rheobase and action potential threshold were unaltered by adolescent DID condition or sex when neurons were held at -70mV. (K) At -70mV, there were significant main effects of sex, adolescent DID, and current injection step on action potential firing. (L-M) Data from (K) graphed separately by sex. Pyramidal neurons from male and female mice which underwent adolescent DID fired fewer action potentials when neurons were held at -70mV. For panels (A-M), n = 9 cells from 5 mice (M DID), 10 cells from 5 mice (F DID), 7 cells from 4 mice (M H2O), and 8 cells from 4 mice (F H2O).

FIGURE 5

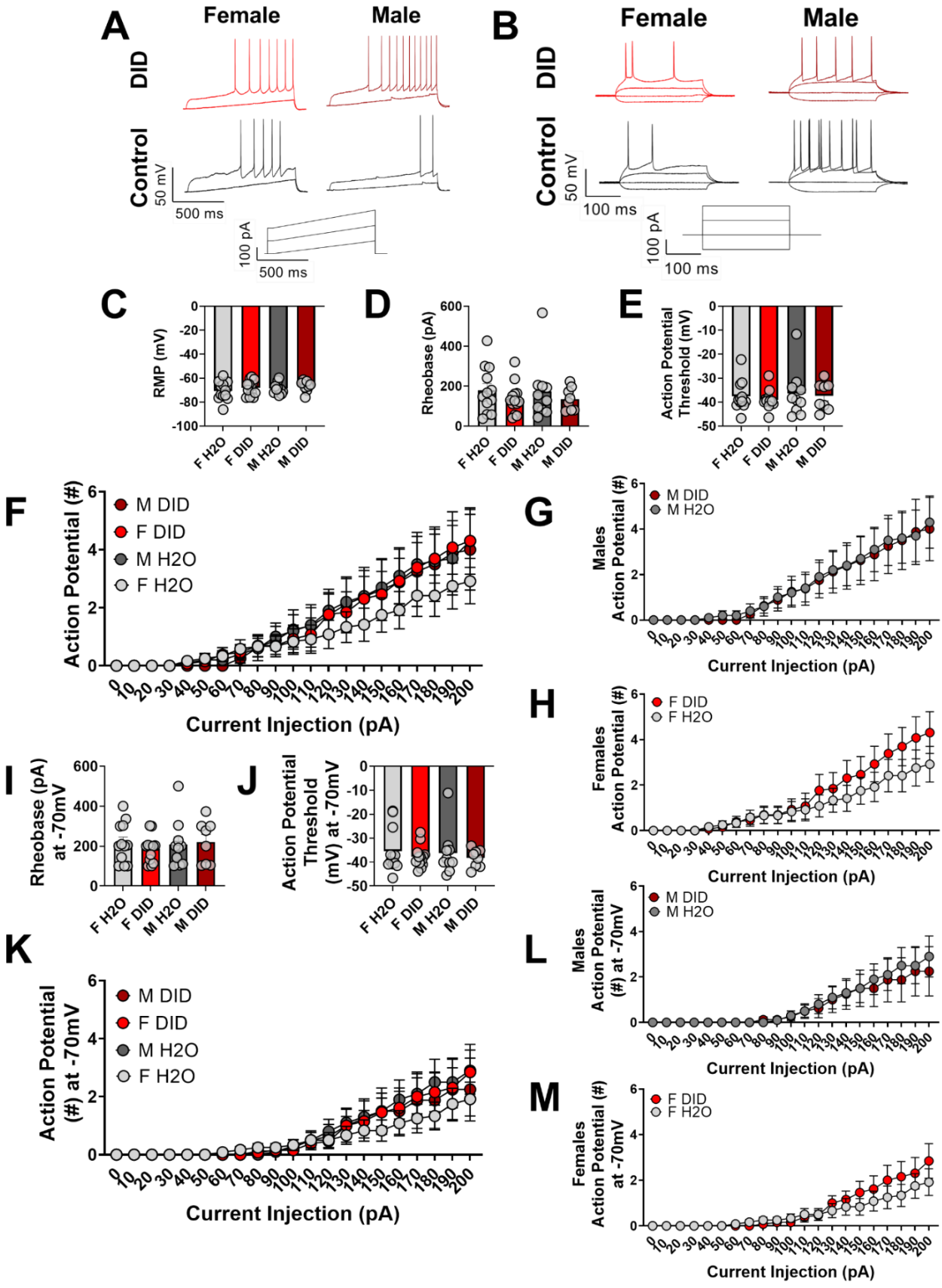

Figure 5. Pyramidal neuron excitability is not altered 30 days after adolescent DID exposure. (A-B) Representative traces for rheobase and VI experiments. (C-E) Pyramidal neuron RMP, rheobase, and action potential threshold are unaltered by adolescent DID and sex. (F) Current-induced action potential firing is not altered in pyramidal neurons by DID or sex 30 days after the cessation of adolescent DID. (G-H) Data from (F) plotted separately by sex for visualization. (I-J) Pyramidal neuron membrane properties are unaltered when held at -70mV. (K) Current-induced firing is not altered by adolescent DID or sex when neurons are held at -70mV. (L-M) Data from (K) graphed separated by sex for visualization. For panels A-L, n = 8 cells from 4 mice (M DID), 13 cells from 8 mice (F DID), 10 cells from 5 mice (M H2O), and 12 cells from 6 mice (F H2O).

FIGURE 6

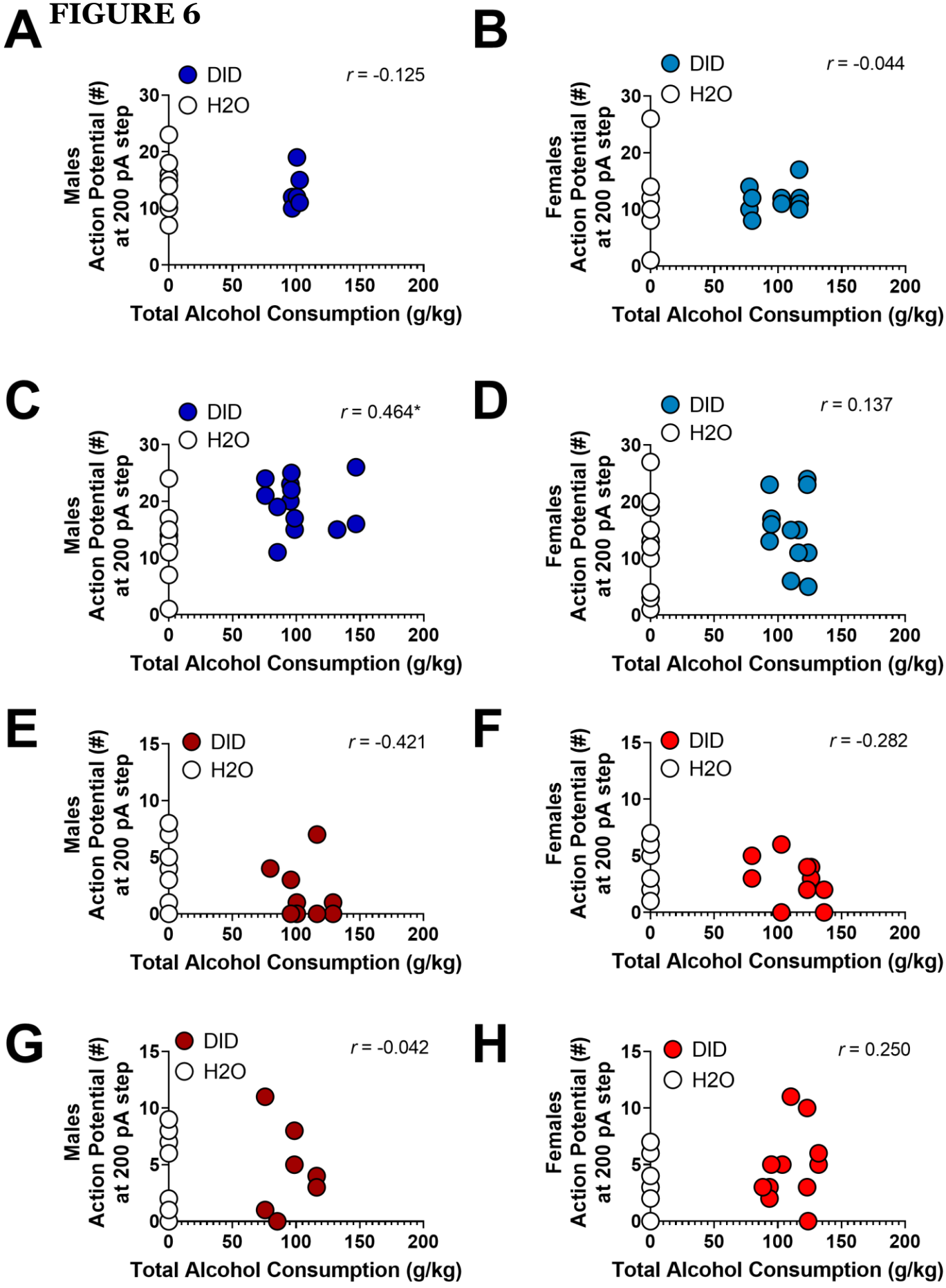

Figure 6. Total alcohol consumption during adolescent DID is correlated with hyperexcitability in adult male mice. (A-B) Total alcohol consumption across 4 cycles of adolescent DID was not significantly correlated with the number of action potentials fired during the final step of VI in SST neurons 24 hr after the end of DID. (C-D) Total alcohol consumption during adolescent DID is positively correlated with hyperexcitability in SST neurons in male mice, but not female mice, 30 days after the cessation of adolescent DID. (E-F) Adolescent alcohol consumption is not correlated with current-induced action potential firing in pyramidal neurons of male or female mice 24 hr after DID. (G-H) Total alcohol consumption during adolescent DID is not significantly correlated with pyramidal neuron action potential firing during the 200 pA step of VI in adult male or female mice.